Perpendicular laser cooling of a rotating ion plasma in a Penning trap

Wayne M. Itano, L. R. Brewer,* D. J. Larson,† and D. J. Wineland
Time and Frequency Division, National Bureau of Standards, Boulder, Colorado 80303
(Received 13 June 1988)

The steady-state temperature of an ion plasma in a Penning trap, cooled by a laser beam perpendicular to the trap axis, has been calculated and measured. The rotation of the plasma, due to crossed **E** and **B** fields, strongly affects the minimum attainable temperature. This is because the velocity distribution of the ions, as seen by a laser beam intersecting the plasma at some distance from the axis of rotation, is skewed, and this leads to a change in the velocity distribution (and hence temperature) at which a steady state is attained. The calculated temperature is a function of the intensity, frequency, and position of the laser beam, and of the rotation frequency of the plasma. Temperatures of $^9Be^+$ plasmas were measured for a wide range of experimental parameters. The lowest and highest temperatures were approximately 40 mK and 2 K. The measured and calculated temperatures are in agreement.

I. INTRODUCTION

Laser cooling is a method by which radiation pressure is used to reduce the temperature of atoms.[1] It has been demonstrated with free and bound atoms and also with ions confined in Paul and Penning traps. Laser cooling of atoms confined by a harmonic potential has been studied theoretically by many methods.[1] The Paul (radiofrequency) trap uses an oscillating, inhomogeneous electric field to create a harmonic potential for the average motion of an ion.[2,3] However, motion in a Paul trap differs from that in a harmonic trap, since there is a forced oscillation (micromotion) at the frequency of the applied field. The micromotion has not been included in calculations of laser cooling, except by numerical simulation.[4]

In a Penning trap, static electric and magnetic fields confine the ions. In some ways, the Penning trap is more difficult than the Paul trap to treat theoretically. Some of the difficulties arise because the electrostatic potential energy decreases as an ion moves radially outward from the trap axis.[2,3] A magnetic field along the trap axis is required to confine the ions radially. The combined effects of the magnetic field and of the radial electric field lead to a circular $\mathbf{E}\times\mathbf{B}$ drift of the ions about the trap axis. This rotation leads to a basic difference between laser cooling in a Penning trap and in a harmonic trap. It can be shown that conservation of energy and of the axial component of the canonical angular momentum L_z guarantees confinement of the ions.[5] However, external torques, due to collisions with neutral molecules or to asymmetries of the trap fields, change L_z and may cause the ions to move outward radially.[6,7] Thus long-term confinement is not guaranteed even if laser cooling reduces the random motion of the ions. A laser beam of appropriate tuning and spatial profile can be used to apply a torque to the ions in order to prevent this radial drift, while also cooling their random motion.[8] The axial motion in a Penning trap does not suffer from these complications, since the axial well is harmonic, and since there are no axial magnetic forces. A laser beam which is not perpendicular to the trap axis can be used to cool this motion.

The previous theoretical treatment of laser cooling in a Penning trap considered only a single ion.[8] When many ions are confined, the additional electric fields lead to an increased rotation frequency of the ions around the axis, which affects the cooling. Also, detailed calculations were carried out only for the case where the Doppler broadening was much smaller than the natural linewidth of the optical transition. This is often not the case in practice.

Several reports of laser cooling of ions in Penning traps have appeared previously.[9–16] While temperature measurements were reported in all of these references, and Ref. 9 reported a measurement of the cooling rate, in rough agreement with theory, very little has been done in the way of quantitative comparisons of theory and experiment. Simple theoretical calculations yield a predicted minimum temperature $T_{\min}=\hbar\gamma_0/2k_B$, where γ_0 is the radiative linewidth of the atomic transition in angular frequency units and k_B is Boltzmann's constant.[8] This minimum temperature has been approached within about a factor of 10 when the laser beam was perpendicular to the trap axis, and within about a factor of 2 when the cooling laser was not perpendicular to the axis.[15] More typically, the lowest observed temperatures were higher than $T_{\min}$ by two orders of magnitude, and no explanation of this discrepancy has been given.

In this paper we present a calculation of the perpendicular (cyclotron) temperature in a Penning trap for the case in which the cooling laser beam is perpendicular to the trap axis. This geometry is often used experimentally.[9,10,12–14] The calculations are compared to experiments in which temperatures of $^9Be^+$ plasmas were measured for a wide range of experimental conditions. For typical experimental conditions, the minimum perpendicular temperature is found to be much greater than $T_{\min}=\hbar\gamma_0/2k_B$. The reason stems from the condition that the work done by the laser on the ions be zero in the steady state. The rate at which work is done on an ion of velocity **v** by a force **F**, which in this case is parallel to the direction of propagation of the laser beam, is $\mathbf{F}\cdot\mathbf{v}$. If the laser beam intersects the ion plasma on the side which is receding from the laser due to the rotation of the plasma, $\mathbf{F}\cdot\mathbf{v}$ would tend to be positive. (If it intersects on the other side, the plasma radius expands and there is no steady state.[10]) In order to make the average value $\langle \mathbf{F}\cdot\mathbf{v}\rangle \approx 0$, the frequency of the laser is tuned below resonance, which, because of the Doppler effect, makes $\mathbf{F}$ stronger for ions with $\mathbf{F}\cdot\mathbf{v}<0$ than for ions with $\mathbf{F}\cdot\mathbf{v}>0$. In order to get $\langle \mathbf{F}\cdot\mathbf{v}\rangle \approx 0$, due to cancellation between negative and positive contributions to the average, the width of the velocity distribution must have a certain value, which corresponds to a temperature higher than $T_{\min}$.

II. THEORY

A. Simple theory

In this section a simplified theory of perpendicular laser cooling of an ion plasma in a Penning trap is presented. Some of the simplifying assumptions will be modified in the following sections, in order to obtain quantitative predictions that can be compared with experiment.

The trap is assumed to approximate the ideal Penning trap, which consists of a uniform magnetic field $\mathbf{B}=B\hat{\mathbf{z}}$ superimposed on a static electric potential

$$\phi_T(r,z)=\frac{m\omega_z^2}{4q}(2z^2-r^2) , \tag{1}$$

where m and q are the mass and charge of an ion, and ω_z is the frequency of axial motion of a single ion in the trap. The actual frequency of motion of an individual ion is shifted by the presence of the other ions. Here, r and z are the cylindrical coordinates of a point in the trap.

It is assumed that the plasma rotates about the z axis with a uniform angular frequency ω, that is, without shear. The velocity distribution of the ions is assumed to be a Maxwell-Boltzmann distribution superimposed on this uniform rotation. A Maxwell-Boltzmann velocity distribution superimposed on a uniform rotation is a characteristic of a non-neutral plasma in thermal equilibrium in cylindrically symmetric fields.[17,18] If there is shear within the plasma, a resulting frictional force tends to reduce the shear, leading to uniform rotation in the steady state. Approximate uniform rotation of the plasmas has been verified experimentally.[12,15,19,20] The temperatures $T_\perp$ and $T_\parallel$ describe the velocity distributions in the x-y plane in the z direction, and differ because cooling of the z motion occurs only by ion-ion collisions. If there were no relaxation between $T_\perp$ and $T_\parallel$, then $T_\parallel$ would increase without limit, due to heating by photon recoil. We assume that the relaxation is sufficient that $T_\parallel$ reaches a steady value somewhat higher than $T_\perp$. Under the assumptions stated in this section, the calculation of $T_\perp$ does not require any knowledge of $T_\parallel$. If the beam is not perpendicular to the axis, the temperatures depend on the relaxation rate between the perpendicular and parallel kinetic energies, which could be measured by a separate experiment.

A key assumption in the calculation of $T_\perp$ is that, except for the change in energy due to the scattering of photons from the laser, the total (kinetic plus potential) energy of the ion plasma is conserved. This is true to the extent that the plasma is isolated from the rest of the universe and can be described by a time-independent Hamiltonian. These assumptions would be violated by collisions of the ions with neutral atoms or by interactions with time-varying external electric and magnetic fields. In practice, the pressure in the trap and the time-varying fields (due, for example, to thermal radiation or to charges moving on the trap electrodes) can be made low enough that the interaction with the laser is the main source of energy change of the ion system. The rapid heating of the ion plasma that was observed in one experiment after the cooling laser was shut off[21] can be accounted for by a conversion of the electrostatic potential energy of the ions to kinetic energy as the plasma expanded radially.

On the other hand, it is *not* assumed that L_z is conserved in the absence of the torque due to the interaction with the laser. If the trap fields were perfectly axially symmetric, and if the ions were totally isolated from collisions with neutral atoms and the radiation field, then L_z would be conserved. However, static electric or magnetic fields which violate axial symmetry can apply a net torque to the ion plasma and change L_z, even though, being time independent, they cannot transfer energy. In fact, such torques are required in order for the plasma to attain a steady state (a state in which all of the observable properties are constant in time) while the laser beam is applying a finite torque to the plasma. It has been experimentally observed that a steady state can be obtained even when the radial displacement of the laser beam from the trap center is greater than the beam radius. In this case, the torque due to the laser must be balanced by the other external torques. The oscillations that have been observed in the fluorescence of a plasma of laser-cooled Mg^+ ions[13] may be due to the fact that the nature of the external torque is such that the energy and the angular momentum cannot be balanced at the same time, for those experimental conditions.

The calculation of the torque applied by the laser is straightforward.[6] The torque due to static field asymmetries is not well understood in general and is a topic of current experimental[6,7,22–25] and theoretical[26,27] research. In studies of confined electron plasmas, it has been observed that, at sufficiently low pressures, the radial expansion rate, which is a measure of the external torque, is independent of the pressure.[7] The expansion rate decreased when care was taken to reduce asymmetries in the apparatus.[22] Some plasma instabilities which can be driven by static field asymmetries have been studied experimentally.[23,24] No attempt will be made in this article to calculate the external torque. Rather, it is assumed that values of ω and $T_\perp$ that ensure a steady state can be found. The point of the calculation is to determine the value of $T_\perp$ which is consistent with given values of ω and the other parameters. In the experiments, ω and $T_\perp$ were varied by varying the position, intensity, and frequency of the cooling laser beam.

The ion plasma is assumed to interact with a monochromatic laser beam, whose frequency ω_L is close to resonance with a strong optical transition of frequency ω_0. We assume that the upper state of the transition decays only to the ground state. The center of the beam lies in the plane defined by $z=0$, and passes through the point $(x,y,z)=(0,d,0)$, parallel to the x axis (see Fig. 1). The coordinate system is such that, for $d>0$, the rotation of the plasma causes the ions to recede from the laser. The laser intensity is assumed to be so low that saturation of the transition can be neglected. The interaction of the ions with the laser radiation is assumed to consist of a series of photon-scattering events. The events are assumed to occur at random times; hence small effects such as photon antibunching[28-33] are neglected here. The delay between the photon absorption from the laser beam and the subsequent photon emission is neglected. This is justified as long as the natural linewidth of the transition is much greater than the frequencies of motion of the ion. (This case has been called the "weak binding" or "heavy particle" limit.[1]) The change in kinetic energy due to scattering a photon depends on the direction of the emitted photon. The angular distribution of the emitted photons, in a frame moving with the atom, is such that the probability of emission in the direction $\hat{\mathbf{k}}$ is equal to the probability of emission in the direction $-\hat{\mathbf{k}}$. The energy change per scattering event, averaged over all possible emission directions, is then

$$\langle \Delta E_K \rangle = \hbar \mathbf{k}\cdot\mathbf{v} + 2R \ , \tag{2}$$

where $\mathbf{k}$ is the wave vector of the absorbed photon ($|\mathbf{k}|=\omega_L/c$), $\mathbf{v}$ is the velocity of the ion before the scattering event, and the recoil energy $R=(\hbar k)^2/(2m)$ [see Eq. (3) of Ref. 34]. This quantity can be thought of as the time integral for one scattering event, of $\mathbf{F}\cdot\mathbf{v}$, including the average effect of the photon recoil.

The rate of energy change of an ion while it is within the laser beam is equal to the product of the average energy change per photon scattering [Eq. (2)] and the rate of photon scatterings. The rate of photon scatterings (in the low-intensity limit) is

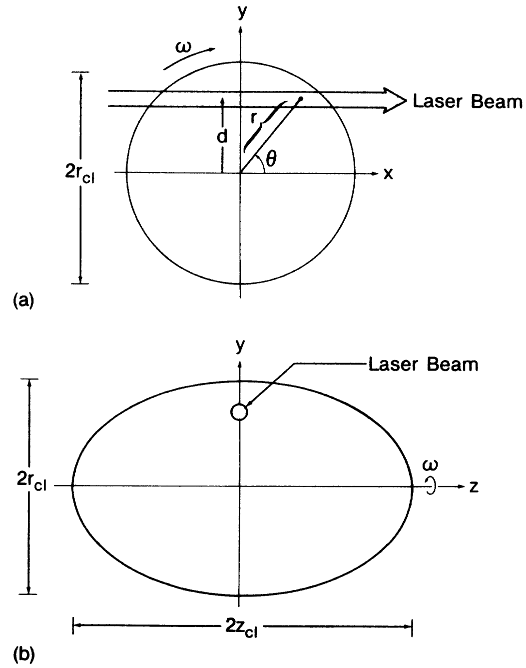

FIG. 1. Diagram showing the laser beam intersecting the ion plasma in (a) the x-y plane and (b) the y-z plane. The laser beam is parallel to the x axis and lies in the $z=0$ plane. Its distance of closest approach to the z axis is d. The direction of the plasma rotation (at angular frequency ω) is indicated.

$$\gamma_L = \frac{I\sigma_0}{\hbar\omega_L}\frac{(\gamma_0/2)^2}{[(\gamma_0/2)^2+\Delta^2]} \ , \tag{3}$$

where I is the light intensity, σ_0 is the scattering cross section at resonance, γ_0 is the natural linewidth of the transition, and $\Delta \equiv \omega_L - \omega_0' - kv_x$ is the detuning of the laser frequency from resonance, taking into account the Doppler shift. Here, $\omega_0' \equiv \omega_0 + R/\hbar$ is the resonance absorption frequency of the ion, which is slightly shifted by the recoil term $R/\hbar$. The velocity-averaged rate of energy change of an ion in the beam is

$$\left\langle \frac{dE}{dt} \right\rangle = \frac{I\sigma_0}{\hbar\omega_L}\int_{-\infty}^{+\infty} \frac{(\hbar k v_x + 2R)\exp[-(v_x-\omega d)^2/u^2]}{\{1+[(2/\gamma_0)(\omega_L-\omega_0'-kv_x)]^2\}\sqrt{\pi}u} dv_x \ , \tag{4}$$

where $u=(2k_B T_\perp/m)^{1/2}$. Equation (4) is the same as Eq. (7) of Ref. 34, except that the center of the velocity distribution is shifted from $v_x=0$ to ωd due to the uniform rotation of the plasma. The finite width of the beam has been neglected here, but will be included later. Below, we solve Eq. (4) for the steady state given by $\langle dE/dt \rangle = 0$.

Equation (4) can be put into a form which is more suitable for computation by expressing the integral in terms of the real and imaginary parts of the complex error function $w(X+iY)$, which can be defined, for $Y>0$, by

$$w(X+iY) = \frac{i}{\pi}\int_{-\infty}^{+\infty} \frac{e^{-t^2}}{X+iY-t} dt \ . \tag{5}$$

The real and imaginary parts of $w(X+iY)$ are

$$\begin{aligned} \mathrm{Re}\, w(X+iY) &= \frac{Y}{\pi}\int_{-\infty}^{+\infty} \frac{e^{-t^2}}{(X-t)^2+Y^2} dt \ , \\ \mathrm{Im}\, w(X+iY) &= \frac{1}{\pi}\int_{-\infty}^{+\infty} \frac{(X-t)e^{-t^2}}{(X-t)^2+Y^2} dt \ . \end{aligned} \tag{6}$$

Tables[35] and methods for the numerical approximation[36] of $w(X+iY)$ have been published.

Let the integration variable in Eq. (4) be changed to $t=(v_x-\omega d)/u$, and let $Y=\gamma_0/(2ku)$ and $X=(\omega_L-\omega_0'-k\omega d)/(ku)$. Then

$$\left\langle \frac{dE}{dt} \right\rangle = \frac{I\sigma_0 Y^2}{\hbar\omega_L\sqrt{\pi}} \int_{-\infty}^{+\infty} \frac{[\hbar k(ut+\omega d)+2R]e^{-t^2}}{Y^2+(X-t)^2} dt \ . \tag{7}$$

Replacing t in the numerator of the integrand by $X-(X-t)$, we have

$$\left\langle \frac{dE}{dt} \right\rangle = \frac{I\sigma_0 k Y^2}{\omega_L\sqrt{\pi}} \left[\left[uX+\omega d+\frac{2R}{\hbar k} \right] \int_{-\infty}^{+\infty} \frac{e^{-t^2}}{Y^2+(X-t)^2} dt - u\int_{-\infty}^{+\infty} \frac{(X-t)e^{-t^2}}{Y^2+(X-t)^2} dt \right]$$

$$= \frac{I\sigma_0\sqrt{\pi} k Y}{\omega_L} \left[\left[uX+\omega d+\frac{\hbar k}{m} \right] \mathrm{Re}\, w(X+iY) - uY\, \mathrm{Im}\, w(X+iY) \right] \ . \tag{8}$$

If the values of the rotation frequency ω, the spatial offset d, and the laser frequency detuning $(\omega_L-\omega_0')$ are fixed, then $\langle dE/dt \rangle$ is a function only of u, which is a function of $T_\perp$. The steady-state value of $T_\perp$ (if it exists) is found by solving the equation $\langle dE/dt \rangle(T_\perp)=0$ for $T_\perp$. This equation has been investigated numerically, and solutions have been found to exist for $\omega d \geq 0$ and $(\omega_L-\omega_0')<0$. The steady-state value of $T_\perp$ is a function of ω, d, and $\Delta\omega_L \equiv \omega_L-\omega_0'$. Since ω and d occur only in the combination ωd, $T_\perp$ is a function of only two variables, ωd and $\Delta\omega_L$, for a given transition in a given ion. There is no dependence of $T_\perp$ on the intensity I, since it enters the expression for $\langle dE/dt \rangle$ as an overall factor and thus does not change the solution of the equation $\langle dE/dt \rangle(T_\perp)=0$.

Figure 2 shows $T_\perp$ as a function of $\Delta\omega_L$, for $\omega/2\pi=50$ kHz and for several values of d. The values of m, γ_0, and ω_0 are for the $2s\,^2S_{1/2}$ to $2p\,^2P_{3/2}$ [$\lambda=313$ nm, $\gamma_0=(2\pi)19.4$ MHz] transition of $^9Be^+$. For a given value of $\Delta\omega_L$, $T_\perp$ increases as d increases. Hence the lowest temperatures are obtained by keeping d as small as possible. The curve of $T_\perp$ for $d=0$ is the same as what would be obtained for a nonrotating plasma ($\omega=0$), because of the way $T_\perp$ depends on ωd. It attains a minimum value $T_\perp \approx \hbar\gamma_0/2k_B$ for $\Delta\omega_L \approx -\gamma_0/2$, just as predicted by theories developed for free atoms or for atoms trapped in harmonic wells, where rotation does not have to be considered.[1,34]

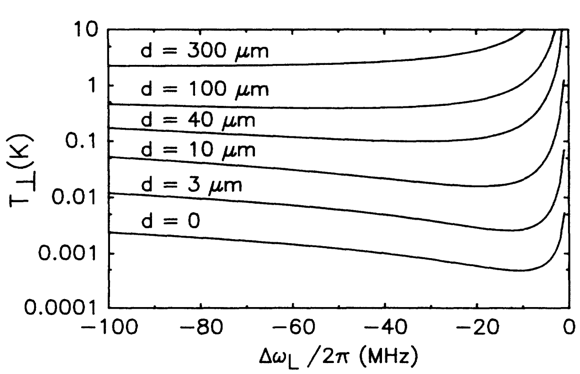

FIG. 2. Graph of the steady-state value of $T_\perp$ for $^9Be^+$ [$\gamma_0=(2\pi)19.4$ MHz, $\lambda=313$ nm] as a function of the laser frequency detuning for several values of the spatial offset d. The rotation frequency $\omega/2\pi$ is 50 kHz. This calculation neglects the finite beam radius and saturation of the optical transition.

We can give a simple explanation for the increase in $T_\perp$ as d increases. In the steady state, $\hbar\mathbf{k}\cdot\mathbf{v}$, averaged over all photon-scattering events, must be negative, in order to balance the $2R$ term in Eq. (2), which is positive. This is done by making $\Delta\omega_L<0$, so that, due to the Doppler shift, there is a preference for ions to scatter photons when $\mathbf{k}\cdot\mathbf{v}<0$. However, for $d>0$, v_x(max), the most probable value of v_x, is shifted to $v_x(\mathrm{max})=\omega d>0$, so that $kv_x(\mathrm{max})>0$. If the width of the v_x distribution, due to the finite value of $T_\perp$, were narrow compared to v_x(max), this would tend to make the average value of $\hbar\mathbf{k}\cdot\mathbf{v}$ positive. The steady state can come about only when the velocity distribution is wide enough that there is a significant probability for an ion to have $\hbar\mathbf{k}\cdot\mathbf{v}<0$. This corresponds to a higher value of $T_\perp$.

Here we make a few remarks about the motion in the z direction. This motion is affected by the recoil of the photons emitted from the ions and by ion-ion collisions. We have assumed that it eventually reaches a steady state, at some $T_\parallel$, and that there is no additional source of heating or cooling for the z motion. Then Eq. (4) contains all of the contributions to dE/dt, since all of the recoil energy is contained in the term $\hbar\mathbf{k}\cdot\mathbf{v}+2R$, and since the total energy of the ion plasma is conserved in collisions between the ions. Thus Eq. (4) can be used to derive the steady-state value of $T_\perp$, and this value does not depend on the final value of $T_\parallel$.

B. Saturation effects

Equation (4) is valid only in the limit that the laser intensity I is low. To generalize it to arbitrary intensity, the expression for the average scattering rage [Eq. (3)] is replaced by[37]

$$\gamma_L = \frac{I\sigma_0}{\hbar\omega_L} \frac{(\gamma_0/2)^2}{[(\gamma/2)^2+\Delta^2]} \ , \tag{9}$$

where γ is the power-broadened linewidth, given by

$$\gamma = \gamma_0\sqrt{1+2S} \ . \tag{10}$$

The saturation parameter S is related to the intensity by

$$S=\frac{I\sigma_0}{\hbar\omega_0\gamma_0} . \tag{11}$$

As stated previously, we ignore the correlations between photon emissions of an ion, which result in photon antibunching. In more sophisticated treatments of laser cooling, which have not yet been applied to the Penning trap, these correlations lead to a modification of the diffusion constant which enters into the equation that describes the evolution of the distribution function of the ions.[28–33] Javanainen[32] has shown that this correction to the diffusion constant can affect the final temperature of laser-cooled ions in a harmonic trap by as much as 20% at high intensities. It has no effect in the limit of low intensities. We do not include it here, since it would complicate the calculations without greatly increasing the accuracy.

Using the power-broadened line shape [Eq. (9)] in place of the low-intensity line shape [Eq. (3)], we find that the average rate of energy change of an ion in the beam is

$$\left\langle \frac{dE}{dt} \right\rangle = \frac{I\sigma_0\gamma_0^2}{\hbar\omega_L\gamma^2}\int_{-\infty}^{+\infty}\frac{(\hbar k v_x+2R)\exp[-(v_x-\omega d)^2/u^2]}{\{1+[(2/\gamma)(\omega_L-\omega_0'-kv_x)]^2\}\sqrt{\pi}u}dv_x . \tag{12}$$

Aside from an overall multiplicative factor, which does not affect the solution of the equation $\langle dE/dt\rangle(T_\perp)=0$, the only difference between Eq. (12) and Eq. (4) is the replacement of the natural radiative linewidth γ_0 by the power-broadened linewidth γ.

Figure 3 shows $T_\perp$ as a function of $\Delta\omega_L$ for several values of S. The other parameters are $\omega/2\pi=50$ kHz and $d=50$ μm. The lowest temperature for a given frequency detuning is obtained by minimizing S.

C. Finite beam geometry

Up to now, the finite radius of the laser beam has been neglected. In this section we investigate its effect on the steady-state temperature.

The average scattering rate at each point in the plasma depends on the intensity at that point through Eq. (9). Let $n(x,y,z)$ be the time-averaged density (ions per unit volume) at the point (x,y,z). Then the rate of change of the total energy of the ion plasma is

$$\left\langle \frac{dE_{\text{tot}}}{dt} \right\rangle = \frac{\sigma_0\gamma_0^2}{\hbar\omega_L}\int_{-\infty}^{+\infty}dx\int_{-\infty}^{+\infty}dy\int_{-\infty}^{+\infty}dz\int_{-\infty}^{+\infty}dv_x I(x,y,z)n(x,y,z)\frac{(\hbar k v_x+2R)\exp[-(v_x-\omega y)^2/u^2]}{\{1+[(2/\gamma)(\omega_L-\omega_0'-kv_x)]^2\}\sqrt{\pi}u\gamma^2} . \tag{13}$$

The linewidth γ is a function of position through its dependence on I, and the fixed spatial offset d of Eq. (4) is replaced by the position variable y.

In the following, we assume that the laser beam is Gaussian, propagates in the $\hat{\mathbf{x}}$ direction, and has its focus at $(x,y,z)=(0,d,0)$. We allow the beam radii w_y and w_z in the radial (y) and axial (z) directions to be different, since this was sometimes the case experimentally. The intensity is then

$$I(y,z)=I_0\exp[-2(y-d)^2/w_y^2-2z^2/w_z^2] , \tag{14}$$

where $I_0=2P/(\pi w_y w_z)$ and where P is the total power in the beam. We neglect the variation of w_y and w_z with x, since, in our experiments, it was small over the size of the plasma. The confocal parameter $b=\pi w^2/\lambda$, which is the distance from the focus at which the beam radius w grows by a factor of $\sqrt{2}$, was typically much greater than the radius of the plasma.

In a continuum model, at low temperatures, the density of a non-neutral plasma is uniform, except for a region on the outer surface whose thickness is on the order of the Debye length.[18] For a non-neutral plasma, the Debye length is defined by[18]

$$\lambda_D\equiv\left[\frac{k_BT}{4\pi n_0 q^2}\right]^{1/2} , \tag{15}$$

where n_0 is the ion density and T is the temperature. For the plasmas studied here, we had $T\leq 2$ K and $n_0\geq 2\times10^7$ ions/cm^3, so that $\lambda_D\leq 20$ μm. Since the plasmas studied typically had diameters greater than 500

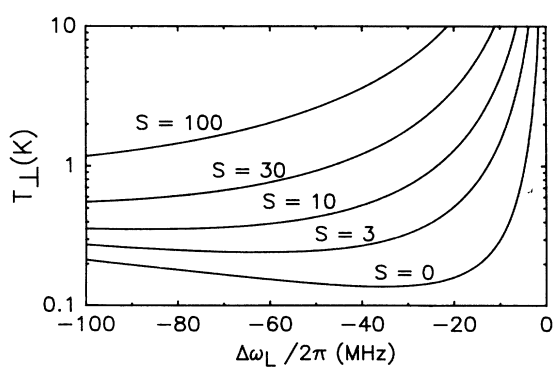

FIG. 3. Graph of the steady-state value of $T_\perp$ for $^9Be^+$ as a function of the laser frequency detuning for several values of the saturation parameter S. The rotation frequency $\omega/2\pi$ is 50 kHz and the spatial offset is 50 μm. This calculation neglects the finite beam radius.

μm, the density can be considered to be uniform. The plasma is a spheroid, whose aspect ratio can be calculated from ω.[6,15] It has been shown theoretically[38] and recently confirmed experimentally[39] that, at very low temperatures, ions in a Penning trap form concentric shells. However, this spatial ordering should have little net effect on the cooling and is ignored here. We assume that the plasma has a uniform density n_0 inside a spheroid of diameter $2r_{\rm cl}$ in the $z=0$ plane and axial extent $2z_{\rm cl}$ and is zero otherwise.

We also assume that the beamwidth is small compared to the plasma dimensions. With these approximations, Eq. (13) is reduced to

$$\left\langle \frac{dE_{\rm tot}}{dt} \right\rangle = \frac{2I_0\sigma_0\gamma_0^2 n_0}{\hbar\omega_L}(r_{\rm cl}^2-d^2)^{1/2}\int_{-\infty}^{+\infty}dy\int_{-\infty}^{+\infty}dz\int_{-\infty}^{+\infty}dv_x\,\exp[-2(y-d)^2/w_y^2-2z^2/w_z^2] \times \frac{(\hbar k v_x+2R)\exp[-(v_x-\omega y)^2/u^2]}{\{1+[(2/\gamma)(\omega_L-\omega_0'-kv_x)]^2\}\sqrt{\pi}u\gamma^2}\ . \quad (16)$$

Here, $2(r_{\rm cl}^2-d^2)^{1/2}$ is the length over which the laser beam intersects the plasma. The v_x integration can be expressed in terms of the complex error function, leaving a two-dimensional integration to be done numerically:

$$\left\langle \frac{dE_{\rm tot}}{dt} \right\rangle = \frac{2I_0\sigma_0 n_0\sqrt{\pi}kuY_0^2}{\omega_L}(r_{\rm cl}^2-d^2)^{1/2}\int_{-\infty}^{+\infty}dy\int_{-\infty}^{+\infty}dz\,\exp[-2(y-d)^2/w_y^2-2z^2/w_z^2] \times \left[\frac{(uX+\omega y+\hbar k/m)}{uY(y,z)}{\rm Re}w(X+iY)-{\rm Im}w(X+iY)\right]\ . \quad (17)$$

Here, $Y_0=\gamma_0/(2ku)$, $X(y)=(\omega_L-\omega_0'-k\omega y)/(ku)$, and $Y(y,z)=\gamma(y,z)/(2ku)$. For a given set of parameters, the equation $\langle dE_{\rm tot}/dt\rangle(T_\perp)=0$ is solved for $T_\perp$. For some ranges of parameters, no solution can be found. This occurs when d is too small relative to w_y, so that the beam has too much intensity on the $y<0$ side of the plasma.

Figure 4 shows $T_\perp$ as a function of $\Delta\omega_L$ for $\omega/2\pi=50$ kHz and for several values of d in the limit of low laser intensity. The beam radii are given by $w_y=w_z=50$ μm. The values of $T_\perp$ calculated from the simple theory of Sec. II A are shown as dashed lines. The effect of the finite beamwidth is to reduce the effective value of d, resulting in a lower value of $T_\perp$. The effect decreases as d increases. For this example, there is a range of values of $\Delta\omega_L$ for which no solution of the equation $\langle dE_{\rm tot}/dt\rangle(T_\perp)=0$ can be found, when d is less than or equal to about 30 μm.

Figure 5 shows the same for a laser power of 50 μW, which is a typical experimental value. This corresponds to a saturation parameter at the center of the beam of $S=3.85$. The effect of saturation is to increase $T_\perp$. This can be seen by comparing the solid curves of Figs. 4 and 5.

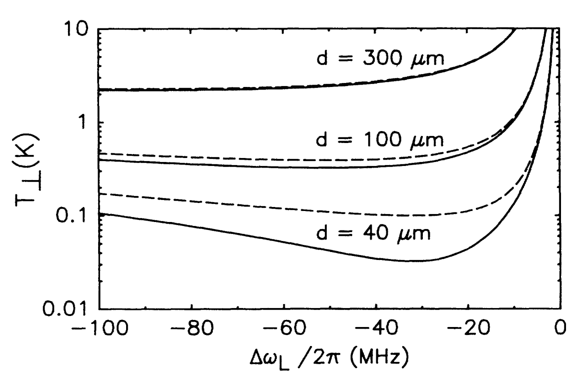

FIG. 4. Graph of the steady-state value of $T_\perp$ for $^9Be^+$ as a function of the laser frequency detuning for several values of d, in the limit of low laser intensity (solid lines). The laser beam is assumed to be Gaussian, with $w_y=w_z=50$ μm. The rotation frequency $\omega/2\pi$ is 50 kHz. The results of the simple theory, which neglects saturation of the optical transition and the finite beam radius, are shown as dashed lines.

III. EXPERIMENT

For the most part, the experimental techniques have been described previously.[12,15] One exception is the abso-

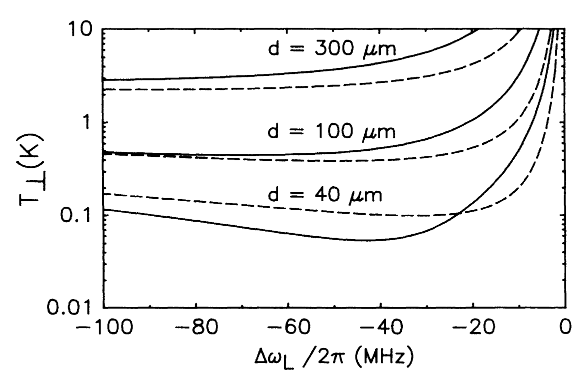

FIG. 5. The same as Fig. 4, except that the laser power is 50 μW. This corresponds to a saturation parameter S at the center of the beam of 3.85.

lute calibration of the laser frequency detuning from resonance $\Delta\omega_L$, which will therefore be described in some detail.

The Penning trap has been described previously.[15,19] It was referred to as trap II in Ref. 15 and has characteristic dimensions $r_0=0.417$ cm and $z_0=0.254$ cm. The operating parameters were $B\approx1.42$ T [cyclotron frequency $\omega_c\approx(2\pi)2.42$ MHz] and $\omega_z\approx(2\pi)213$ kHz (ring-to-endcap voltage $V_0\approx1.5$ V). The $^9Be^+$ ions were loaded into the trap by ionizing neutral Be atoms, evaporated from a filament, with an electron beam. The electrons and the neutral Be atoms entered the trap through holes in the endcaps which were centered on the trap symmetry axis.

Two cw single-mode dye lasers were used in the experiment. Both were frequency doubled to 313 nm in a temperature phase-matched rubidium-dihydrogen-phosphate crystal. The two laser beams were directed though the ion plasma, in opposite directions, perpendicular to the magnetic field. The beams passed through 0.25-cm-diam holes on opposite sides of the ring electrode. One of the laser beams, with a power of approximately 50 μW at 313 nm, was used to cool the ions. The other laser beam, which had much lower power at 313 nm (typically less than 1 μW), was used as a probe, inducing changes in the 313-nm resonance fluorescence light from the cooling beam, from which the temperature and rotation frequency could be derived.[12,15] The backscattered resonance fluorescence light in an $f/6$ cone centered on the cooling beam was collected by a mirror (which had a hole to allow passage of the cooling beam) and focused by a system of lenses onto a photomultiplier tube.

The beams were displaced laterally by lenses attached to micrometer-driven stages. The position of the cooling beam relative to the center of the trap was determined by monitoring the intensity transmitted through the trap as the beam was cut off by the edges of the holes in the electrode. The uncertainty in this determination was estimated to be about 13 μm.

The average frequency of the laser beam used for cooling was kept fixed to about 1 MHz by a servolock to a saturated-absorption resonance in molecular iodine. The laser frequency was modulated over a range of about 16 MHz (at 313 nm), in order to obtain the feedback signal necessary for the lock. To simulate this frequency modulation, an additional integration over $\Delta\omega_L$ could be performed. This would improve the accuracy of the calculations only for small values of $\Delta\omega_L$.

An optical double-resonance method described in detail elsewhere[12,15] was used to measure $T_\perp$. The cooling laser was tuned to the $2s\,^2S_{1/2}(m_I=+\frac{3}{2},\ m_J=+\frac{1}{2})$ to $2p\,^2P_{3/2}(m_I=+\frac{3}{2},\ m_J=+\frac{3}{2})$ transition, hereafter called the cycling transition. This yielded a steady fluorescence signal, since this excited-state sublevel always decayed back to the same ground-state sublevel. The weak probe laser was tuned to drive the depopulation transition from the $2s\,^2S_{1/2}(m_I=+\frac{3}{2},\ m_J=+\frac{1}{2})$ sublevel to the $2p\,^2P_{3/2}(m_I=\frac{3}{2},\ m_J=-\frac{1}{2})$ sublevel, which decayed $\frac{2}{3}$ of the time to the $2s\,^2S_{1/2}(m_I=+\frac{3}{2},\ m_J=-\frac{1}{2})$ ground-state sublevel. This sublevel did not fluoresce, since it was far from resonance with either laser. Population in the $2s\,^2S_{1/2}(m_I=+\frac{3}{2},\ m_J=-\frac{1}{2})$ sublevel was transferred back to the $2s\,^2S_{1/2}(m_I=+\frac{3}{2},\ m_J=+\frac{1}{2})$ sublevel in about 1 s by off-resonance optical pumping from the cooling laser.[12,15] The probe laser resonance was observed in

TABLE I. Comparison of calculated and measured values of $T_\perp$ for perpendicular laser cooling of $^9Be^+$ in a Penning trap, for experimentally determined parameters ω, d, $\Delta\omega_L$, P, w_y, and w_z.

$\omega/2\pi$ (kHz)	d (μm)	$\Delta\omega_L/2\pi$ (MHz)	P (μW)	w_y (μm)	w_z (μm)	$T_{\perp calc}$ (K)	$T_{\perp meas}$ (K)
67.5	127	−29	30	24	24	$3.0^{+2.7}_{-1.3}$	1.9±0.2
99.7	127	−44	49	82	31	$2.0^{+1.0}_{-0.7}$	1.6±0.3
65.7	127	−44	38	82	31	$0.91^{+0.39}_{-0.30}$	1.27±0.10
35.9	165	−78	30	24	24	$0.82^{+0.16}_{-0.15}$	0.96±0.11
36.7	165	−46	30	24	24	$1.05^{+0.35}_{-0.26}$	0.96±0.11
36.3	165	−61	30	24	24	$0.89^{+0.21}_{-0.18}$	0.91±0.08
38.6	51	−13	30	24	24	$0.62^{+10}_{-0.47}$	0.69±0.07
40.0	127	−46	30	24	24	$0.77^{+0.28}_{-0.20}$	0.61±0.05
32.6	127	−80	30	24	24	$0.49^{+0.10}_{-0.09}$	0.55±0.05
35.9	127	−62	30	24	24	$0.57^{+0.15}_{-0.12}$	0.47±0.05
35.0	89	−29	30	24	24	$0.48^{+0.39}_{-0.18}$	0.27±0.03
28.5	89	−63	30	24	24	$0.24^{+0.06}_{-0.06}$	0.25±0.03
28.1	89	−79	30	24	24	$0.25^{+0.06}_{-0.05}$	0.21±0.03
31.0	89	−45	30	24	24	$0.29^{+0.10}_{-0.09}$	0.20±0.02
29.2	76	−55	49	82	31	$0.087^{+0.046}_{-0.042}$	0.13±0.04
23.1	76	−55	49	82	31	$0.075^{+0.032}_{-0.030}$	0.11±0.05
21.6	51	−79	30	24	24	$0.100^{+0.031}_{-0.029}$	0.097±0.020
38.1	64	−44	38	82	31	$0.044^{+0.067}_{-0.044}$	0.085±0.009
29.4	76	−44	49	82	31	$0.084^{+0.051}_{-0.046}$	0.081±0.011
23.8	51	−46	30	24	24	$0.092^{+0.037}_{-0.033}$	0.080±0.020
17.3	64	−44	38	82	31	$0.037^{+0.019}_{-0.017}$	0.043±0.040

the form of a decrease in the fluorescence from the cycling transition as the probe laser was tuned in frequency. The contribution to the width of this resonance from the Doppler broadening was used to derive $T_\perp$. The optical double-resonance method has the advantage of not greatly perturbing the temperature of the plasma. The rotation frequency ω was measured from the shift in the frequency of the center of the depopulation resonance, due to the Doppler shift, for a given translation of the probe beam in the y direction.[12,15]

The absolute calibration of the cooling laser detuning $\Delta\omega_L$ was made by the following method. The magnetic field was fixed at a particular NMR resonance frequency, and the cooling laser was locked to the iodine signal. The edges of the plasma were located with the probe beam by finding the positions at which the double-resonance signal disappeared.[12,15] The probe beam was then positioned at the center of the plasma and tuned to the cycling transition. At the center of the plasma, $d=0$, so the average Doppler shift due to rotation is zero. The increase in fluorescence as the probe laser was tuned across the cycling transition was observed while the cooling laser kept the plasma at a constant temperature. For this measurement the cooling beam was chopped, and the fluorescence was detected while it was off, in order to reduce the background. The probe laser was then tuned to the frequency at which the peak of the cycling resonance occurred. Some of the radiation from each of the two lasers was combined on the surface of a silicon photodiode by means of a beamsplitter. The beat frequency was measured with a radio-frequency spectrum analyzer. This measurement yielded the value of $\Delta\omega_L/2\pi$ with an uncertainty of about 10 MHz (at 313 nm). The value of $\Delta\omega_L$ at other magnetic fields could be calculated from the known Zeeman shift of the resonance line.

IV. RESULTS

Table I summarizes the results of the measurements. The values of $T_\perp$ calculated from the various experimental parameters are shown in the column labeled $T_{\perp\mathrm{calc}}$. They are in good agreement with the values of $T_\perp$ measured from the Doppler broadening of the optical double resonance, which are shown in the column labeled $T_{\perp\mathrm{meas}}$. This agreement is maintained over a wide range of values of d, ω, and $\Delta\omega_L$. The range of values of $T_\perp$ is from about 0.04 K to about 2 K. All of the parameters that go into the calculation are measured, rather than fitted. The uncertainties in $T_{\perp\mathrm{calc}}$ are due to the uncertainties in the parameters ω, d, $\Delta\omega_L$, P, ω_y, and ω_z. In most cases, the uncertainty in d of about 13 μm makes the largest contribution to the uncertainty in $T_{\perp\mathrm{calc}}$. For small values of $\Delta\omega_L$, the uncertainty in $\Delta\omega_L$ of about (2π)10 MHz makes the largest contribution. The uncertainty in ω of about 5% and the uncertainties in P, w_y, and w_z of about 20% make relatively minor contributions. Figure 6 is a scatter plot of the measured values $T_{\perp\mathrm{meas}}$ versus the calculated values $T_{\perp\mathrm{calc}}$. The data points lie close to the dashed line, which denotes the condition $T_{\perp\mathrm{meas}}=T_{\perp\mathrm{calc}}$.

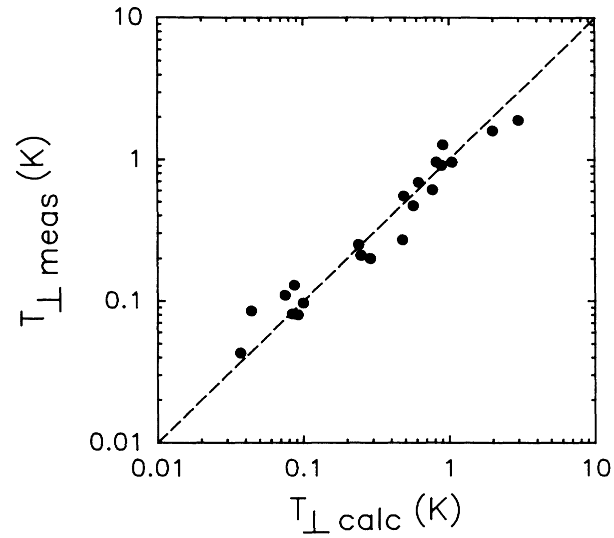

FIG. 6. Scatter plot of measured values of $T_\perp$ (vertical axis) vs calculated values of $T_\perp$ (horizontal axis). The dashed line corresponds to $T_{\perp\mathrm{meas}}=T_{\perp\mathrm{calc}}$.

The observed values of $T_\perp$ are much higher (up to three orders of magnitude) than those predicted by a theory which does not take rotation into account (the $d=0$ curve in Fig. 2). In order to obtain very low temperatures, the cooling laser beam should not be perpendicular to **B**. Low temperatures, approaching the $T_{\min}=\hbar\gamma_0/2k_B$ limit, have been attained for $^9Be^+$ plasmas in Penning traps by supplementing perpendicular cooling with cooling by a beam which was not perpendicular to **B**.[15,39]

A possible configuration for obtaining the lowest possible temperatures is a combination of two laser beams, one to cool the ions and the other to maintain the radial size of the plasma. The strong cooling beam, with a frequency detuning $\Delta\omega_L=-\gamma_0/2$, would be directed along the z axis. If the power in this beam were not too high, then Coulomb coupling between ions would ensure $T_\perp\approx T_\parallel\approx\hbar\gamma_0/2k_B$. The second beam, in the x-y plane, would be positioned to apply a torque to counteract the radial expansion due to external torques and to photon recoil from the cooling beam. The photon-scattering rate from this beam could be made low enough so as not to significantly affect the overall temperature.

ACKNOWLEDGMENTS

We gratefully acknowledge the support of the U.S. Office of Naval Research and the U.S. Air Force Office of Scientific Research. One of us (D.J.L.) acknowledges partial support of the National Science Foundation. We thank J. C. Bergquist, J. J. Bollinger, and S. L. Gilbert for carefully reading the manuscript.

*Present address: L250, Lawrence Livermore National Laboratory, Livermore, CA 94550.
†Permanent address: Department of Physics, University of Virginia, Charlottesville, VA 22901.

[1]For recent reviews of laser cooling, see D. J. Wineland and W. M. Itano, Phys. Today **40**(6), 34 (1987); S. Stenholm, Rev. Mod. Phys. **58**, 699 (1986).
[2]H. G. Dehmelt, Adv. At. Mol. Phys. **3**, 53 (1967).
[3]D. J. Wineland, W. M. Itano, and R. S. Van Dyck, Jr., Adv. At. Mol. Phys. **19**, 135 (1983).
[4]R. Casdorff and R. Blatt, Appl. Phys. B **45**, 175 (1988); J. Hoffnagle, R. G. DeVoe, L. Reyna, and R. G. Brewer, Phys. Rev. Lett. **61**, 255 (1988); R. Blümel, J. M. Chen, E. Peik, W. Quint, W. Schleich, Y. R. Shen, and H. Walther, Nature (London) **334**, 309 (1988).
[5]T. M. O'Neil, Phys. Fluids **23**, 2216 (1980).
[6]D. J. Wineland, J. J. Bollinger, W. M. Itano, and J. D. Prestage, J. Opt. Soc. Am. B **2**, 1721 (1985).
[7]C. F. Driscoll and J. H. Malmberg, Phys. Rev. Lett. **50**, 167 (1983).
[8]W. M. Itano and D. J. Wineland, Phys. Rev. A **25**, 35 (1982).
[9]D. J. Wineland, R. E. Drullinger, and F. L. Walls, Phys. Rev. Lett. **40**, 1639 (1978).
[10]R. E. Drullinger, D. J. Wineland, and J. C. Bergquist, Appl. Phys. **22**, 365 (1980).
[11]D. J. Wineland and W. M. Itano. Phys. Lett. **82A**, 75 (1981).
[12]J. J. Bollinger and D. J. Wineland, Phys. Rev. Lett. **53**, 348 (1984).
[13]R. C. Thompson, G. P. Barwood, and P. Gill, Opt. Acta **33**, 535 (1986); Appl. Phys. B **46**, 87 (1988).
[14]F. Plumelle, M. Desaintfuscien, M. Jardino, and P. Petit, Appl. Phys. B **41**, 183 (1986).
[15]L. R. Brewer, J. D. Prestage, J. J. Bollinger, W. M. Itano, D. J. Larson, and D. J. Wineland, Phys. Rev. A **38**, 859 (1988).
[16]R. G. Hulet, D. J. Wineland, J. C. Bergquist, and W. M. Itano, Phys. Rev. A **37**, 4544 (1988).
[17]R. C. Davidson, *Theory of Nonneutral Plasmas* (Benjamin, Reading, MA, 1974).
[18]T. M. O'Neil and C. F. Driscoll, Phys. Fluids **22**, 266 (1979); S. A. Prasad and T. M. O'Neil, *ibid.* **22**, 278 (1979).
[19]D. J. Larson, J. C. Bergquist, J. J. Bollinger, W. M. Itano, and D. J. Wineland, Phys. Rev. Lett. **57**, 70 (1986).
[20]C. F. Driscoll, J. H. Malmberg, and K. S. Fine, Phys. Rev. Lett. **60**, 1290 (1988).
[21]J. J. Bollinger, J. D. Prestage, W. M. Itano, and D. J. Wineland, Phys. Rev. Lett. **54**, 1000 (1985).
[22]C. F. Driscoll, K. S. Fine, and J. H. Malmberg, Phys. Fluids **29**, 2015 (1986).
[23]D. L. Eggleston, T. M. O'Neil, and J. H. Malmberg, Phys. Rev. Lett. **53**, 982 (1984).
[24]D. L. Eggleston and J. H. Malmberg, Phys. Rev. Lett. **59**, 1675 (1987).
[25]J. Yu, M. Desaintfuscien, and F. Plumelle, in *Laser Spectroscopy VIII*, Vol. 55 of Springer Series in Optical Sciences, edited by W. Persson and S. Svanberg (Springer, Berlin, 1987), p. 75.
[26]J. D. Crawford, T. M. O'Neil, and J. H. Malmberg, Phys. Rev. Lett. **54**, 697 (1985).
[27]J. D. Crawford and T. M. O'Neil, Phys. Fluids **30**, 2076 (1987).
[28]R. J. Cook, Opt. Commun. **35**, 347 (1980).
[29]J. P. Gordon and A. Ashkin, Phys. Rev. A **21**, 1606 (1980).
[30]R. J. Cook, Phys. Rev. A **22**, 1078 (1980).
[31]V. G. Minogin, Zh. Eksp. Teor. Fiz. **79**, 2044 (1980) [Sov. Phys.—JETP **52**, 1032 (1980)].
[32]J. Javanainen, J. Phys. B **14**, 4191 (1981).
[33]S. Stenholm, Phys. Rev. A **27**, 2513 (1983).
[34]D. J. Wineland and W. M. Itano, Phys. Rev. A **20**, 1521 (1979).
[35]V. N. Faddeyeva and N. M. Terent'ev, *Tables of Values of the Function* $w(z)=e^{-z^2}[1+(2i/\sqrt{\pi})\int_0^z e^{t^2}dt]$ *for Complex Argument,* translated by D. G. Fry (Pergamon, New York, 1961); B. D. Fried and S. D. Conte, *The Plasma Dispersion Function* (Academic, New York, 1961).
[36]See, for example, A. K. Hui, B. H. Armstrong, and A. A. Wray, J. Quant. Spectrosc. Radiat. Transfer **19**, 509 (1978); J. Humlíček, *ibid.* **21**, 309 (1979).
[37]See, for example, W. Demtröder, in *Laser Spectroscopy,* Vol. 5 of Springer Series in Chemical Physics, edited by V. I. Goldanskii, R. Gomer, F. P. Schäfer, and J. P. Toennies (Springer, Berlin, 1982), p. 105.
[38]D. H. E. Dubin and T. M. O'Neil, Phys. Rev. Lett. **60**, 511 (1988).
[39]S. L. Gilbert, J. J. Bollinger, and D. J. Wineland, Phys. Rev. Lett. **60**, 2022 (1988).